Biotechnology and Bioengineering

WILEY

BIOTECHNOLOGY AND BIOENGINEERING

ARTICLE

Resistive Method for Bacterial Detection Employing a Silicon Nanowire Electrical Chip

Alexander S. Ilin[1] | Mikhail N. Martyshov[1] | Dmitrii V. Gusev[1] | Daniil M. Rusakov[1] | Daria A. Nazarovskaia[1] | Pavel A. Domnin[2] | Mengyuan Wang[1] | Ilia I. Tsiniaikin[1] | Kirill A. Gonchar[1] | Svetlana A. Ermolaeva[2] | Liubov A. Osminkina[1] | Pavel A. Forsh[1]

[1]Faculty of Physics, Lomonosov Moscow State University, Moscow, Russia | [2]N.F. Gamaleya Federal Research Center for Epidemiology and Microbiology, Moscow, Russia

Correspondence: Alexander S. Ilin (ilinas@my.msu.ru; as.ilin@physics.msu.ru) | Liubov A. Osminkina (osminkina@physics.msu.ru) | Pavel A. Forsh (phorsh@mail.ru)

Received: 14 October 2024 | **Revised:** 13 January 2025 | **Accepted:** 12 February 2025

Funding: The study was supported by the Russian Science Foundation, grant no. 22-72-10062.

Keywords: bacterial detection | electrical chip | impedance spectroscopy | Listeria | silicon nanowires

ABSTRACT

There is now an urgent need to develop reliable, rapid, and cost-effective methods for bacterial detection, particularly for point-of-care applications. This study explores the unique properties of silicon nanowire (SiNW) arrays as a resistive sensing platform for detecting *Listeria innocua*. Vertically aligned SiNWs, fabricated via metal-assisted chemical etching, exhibited high sensitivity to bacterial adsorption. Conductance measurements revealed a more than 10-fold increase as bacterial concentrations rose from 10^5 to 10^7 CFU/mL, with clear saturation at higher levels. The study employed both direct current (DC) and alternating current (AC) methodologies, with AC conductance consistently outperforming DC due to reduced potential barrier effects. An equivalent circuit model was developed to describe the impedance behavior of the SiNW-bacteria system, offering valuable insights into charge transport mechanisms. These results demonstrate the potential of SiNW-based sensors as robust, scalable, and high-performance diagnostic tools. Beyond bacterial detection, the proposed platform offers promising applications in clinical diagnostics, environmental monitoring, and food safety.

1 | Introduction

Despite significant advancements in the control of infectious diseases, several infections continue to pose considerable challenges for accurate and timely diagnosis. One such infection is listeriosis, a severe condition caused by the bacterium *Listeria monocytogenes*. Commonly found in contaminated food, this pathogen can lead to serious health complications, including meningitis, encephalitis, septicemia, endocarditis, abscesses, and purulent lesions (Allerberger and Wagner 2010). The incidence of listeriosis has been steadily increasing, making it a growing public health concern in the 21st century. Alarmingly, the disease is associated with a high mortality rate, with approximately 20% of infected individuals succumbing to its effects (Oevermann et al. 2010; Zhang et al. 2021).

The rapid and reliable detection of pathogenic bacteria remains a critical challenge in medical diagnostics, food safety, and environmental monitoring. Traditional methods, such as culture techniques, though highly sensitive, are time-consuming and labor-intensive, requiring 24–72 h for conclusive results. Molecular approaches, such as polymerase chain reaction, offer faster detection times but require specialized equipment and trained personnel, limiting their accessibility in decentralized settings. This underscores the need for advanced biosensor technologies capable of rapid, sensitive, and cost-effective bacterial detection.

Biosensors have emerged as versatile tools for bacterial detection due to their ability to convert biological interactions into measurable physical or chemical signals. Among the various

types, optical sensors, such as surface plasmon resonance devices, are renowned for their high accuracy in detecting target bacteria through changes in optical properties. However, these systems often rely on bulky and expensive instrumentation, as well as strict environmental controls, which restrict their use in field applications. Piezoelectric sensors offer real-time detection by monitoring changes in oscillation frequencies upon bacterial binding, yet they typically require extended incubation times and complex surface regeneration protocols. Electrochemical sensors, including impedance-based devices, provide a promising alternative by enabling label-free, direct detection of bacterial interactions. Despite these advances, each technology faces challenges in balancing sensitivity, simplicity, and scalability for widespread application (Kotsiri et al. 2022; Ahmed et al. 2014; Ivnitski et al. 1999).

For addressing infections caused by pathogenic *Listeria*, it is crucial to understand the structural and functional biology of these bacteria. *Listeria monocytogenes*, the primary pathogenic species, is distinguished by its production of internalin B (InlB), a surface protein that facilitates phagocytosis and hepatocyte invasion, driving its virulence (Chalenko et al. 2017; Ireton et al. 2021). Detecting InlB in body fluids such as blood plasma or urine could serve as a specific biomarker for early listeriosis diagnosis. However, existing serological methods often suffer from high rates of false positives and negatives, along with limited sensitivity and specificity (Lopes-Luz et al. 2021). These shortcomings underscore the need for advanced diagnostic tools that can provide accurate, early detection of listeriosis, ultimately improving patient outcomes through timely intervention.

One promising approach for detecting *Listeria* and other pathogens is the use of resistive biosensors, which have gained popularity due to their simplicity and effectiveness. These sensors operate by measuring changes in the electrical resistance of a sensing material upon interaction with target entities, such as bacteria (Flammini et al. 2004). The straightforward construction and operation of resistive sensors have contributed to their widespread application in diverse fields, including medical diagnostics and environmental monitoring (De Boer et al. 2007; Ilyin et al. 2015; Ilin et al. 2017; Filatova and Rumyantseva 2023).

A key factor in the performance of resistive biosensors is the specific surface area of the sensing material. Low-dimensional systems with nanostructured morphologies offer a significant advantage by providing a highly increased surface area. This enhancement improves sensor sensitivity, enabling the detection of low concentrations of biological targets—an essential feature in clinical diagnostics (Feng et al. 2021; Xu et al. 2020; Levitsky 2015; Archer et al. 2005; Gupta and Gupta 2005; Daraee et al. 2016; Osminkina et al. 2022; Forsh et al. 2007; Martyshov et al. 2009; Forsh et al. 2008; Gongalsky et al. 2020; Gonchar et al. 2020; Nazarovskaia et al. 2023). Additionally, resistive chemical sensors based on low-dimensional systems can operate at reduced temperatures, require minimal power, and are adaptable to a variety of application conditions, making them highly versatile. Their ease of fabrication and the relatively low cost of the materials further solidify their appeal as next-generation chemical sensors.

Among the various materials used in biosensor fabrication, nanocrystalline silicon has emerged as a particularly promising candidate due to its unique chemical and physical properties. The nanostructured surface of silicon offers exceptional sensitivity and selectivity for detecting a broad range of targets, including gases, organic compounds, and biomolecules (Archer et al. 2005; Osminkina et al. 2022; Forsh et al. 2007; Martyshov et al. 2009; Forsh et al. 2008; Gongalsky et al. 2020; Gonchar et al. 2020; Nazarovskaia et al. 2023). For example, porous silicon, with its high specific surface area, significantly enhances the number of active sites available for analyte interaction, thereby improving sensor performance (Forsh et al. 2007; Martyshov et al. 2009; Forsh et al. 2008).

Silicon nanowires (SiNWs) have emerged as a promising platform for bacterial detection, leveraging their unique morphological features, such as high surface-to-volume ratios and well-ordered structures. These characteristics enhance bacterial adhesion and facilitate precise measurement of electrical changes during interactions (Gongalsky et al. 2020; Gonchar et al. 2020; Nazarovskaia et al. 2023). In previous research, SiNW arrays were utilized as sensitive elements to monitor electrical changes caused by bacterial adhesion. For example, Jeong et al. observed that bacterial cells adhered preferentially to nanowire arrays, altering electrical resistance due to the disruption of conductive pathways (Jeong et al. 2013). Similarly, Le Borgne et al. demonstrated that interdigitated electrodes connected by SiNWs exhibited significant resistance changes when bacteria were deposited onto the array. The networked morphology of the SiNW arrays ensured efficient bacterial capture, enabling precise electrical detection (Le Borgne et al. 2018).

In this work, we present a simplified yet highly sensitive resistive platform based on SiNW arrays. The unique morphological properties of these arrays, carefully optimized in our approach, significantly enhance bacterial adsorption and enable precise electrical detection. This method avoids the need for complex processing steps while maintaining high sensitivity and rapid detection capabilities, making it a practical solution for bacterial monitoring systems.

The current study investigates changes in both direct and alternating current (DC and AC) conductivity of SiNW arrays in response to the adsorption of varying concentrations of non-pathogenic bacteria, *Listeria innocua*. Our results demonstrate that SiNW-based sensors offer substantial potential for the rapid and reliable detection of bacteria, paving the way for advanced diagnostic tools. These sensors hold particular promise for clinical applications, where the swift and accurate identification of pathogenic bacteria is critical for effective treatment and infection control. Furthermore, the principles established in this study extend beyond the detection of *Listeria*, providing a foundation for the development of low-cost, high-performance biosensors applicable across diverse diagnostic scenarios.

2 | Materials and Methods

SiNWs were fabricated using the metal-assisted chemical etching (MACE) method from p-type crystalline silicon (c-Si) with a crystallographic orientation of (100) and a resistivity of 10–20 Ω·cm. Initially, the c-Si substrate was cleaned to remove potential contaminants by sequentially washing it in acetone

and isopropanol in an ultrasonic bath, followed by treatment with 5 M HF to eliminate surface silicon oxide.

The cleaned c-Si was then immersed in a solution of 0.01 M $AuCl_3$ and 5 M HF (1:1 volume ratio) for 15 s, resulting in the deposition of gold nanoparticles (AuNPs) on the silicon surface. Subsequently, the AuNP-coated c-Si was placed in a solution of 5 M HF and 30% H_2O_2 (10:1 volume ratio) for 30 min, where etching occurred in the regions covered by AuNPs. After the etching process, AuNPs were removed by immersing the sample in aqua regia (a mixture of nitric acid (HNO_3) and hydrochloric acid (HCl) in a 3:1 volume ratio) for 5 min.

The SiNWs were prepared at room temperature. Following fabrication, the substrates with nanowires were diced into 0.5×0.5 cm chips for subsequent use in sensor applications.

To investigate the conductivity of the samples and the influence of bacteria on it, aluminum contacts measuring 1.5×3.4 mm were deposited onto SiNW samples (1.2 mm thick) using thermal spraying on a VUP-5 unit. The sputtering process was carefully controlled to ensure that aluminum particles adhered to the surface of the nanowires without penetrating the regions between them, thereby avoiding short circuits between the contacts and the underlying c-Si substrate. To achieve this, the sample was positioned at a 70° angle relative to the aluminum crucible during the deposition process.

The morphology of the obtained SiNWs was studied using a Carl Zeiss SUPRA 40 FE-SEM scanning electron microscope equipped with an Inlens SE detector. The imaging was performed at an accelerating voltage of 10 kV and an aperture size of 30 μm.

The *Listeria innocua* (*L. innocua*) strain SLCC3379 was obtained from the N. F. Gamaleya National Research Center for Epidemiology and Microbiology (Russia) and stored at −70°C in 10% glycerol. The bacteria were cultivated overnight in brain heart infusion (BHI) broth at 37°C under constant shaking at 180 rpm. Following cultivation, the suspension was diluted 1:100 with fresh medium to achieve a concentration of $1.6 \cdot 10^7$ CFU/mL (colony-forming units per milliliter).

For SEM imaging of bacteria adsorbed onto SiNWs, an accelerating voltage of 2 keV was used. Before imaging, the bacteria were immobilized on the SiNW substrates using a 2% glutaraldehyde solution in PBS for 90 min, followed by dehydration through an ethanol series ranging from 50% to absolute ethanol (Nazarovskaia et al. 2023).

To investigate the influence of bacteria on the conductivity of SiNWs, an initial measurement was conducted by placing a drop of distilled water on the sample and recording its conductivity. Subsequently, drops of bacterial suspensions with varying concentrations were applied to the samples. The bacterial suspensions, prepared in distilled water, ranged from 10^5 to 10^7 CFU/mL. This approach allowed for a systematic examination of how bacterial concentration impacts the electrical properties of the SiNW samples.

Schematic representation for obtaining an electrical sensor based on SiNWs is shown in Figure 1.

AC measurements were carried out using an HP 4192 A impedance analyzer, which operates across a wide frequency range of 5 Hz–13 MHz. The amplitude of the applied AC voltage was set to 0.05 V to ensure precise impedance characterization. For DC measurements, a Keithley 6487 source picoammeter was employed, offering high sensitivity and accuracy for evaluating the electrical properties of the samples.

3 | Results and Discussion

Figure 2 shows SEM micrographs of SiNWs, which appear as quasi-ordered arrays of nanowires predominantly oriented along the [100] crystallographic direction. The thickness of the SiNW layer after etching is approximately 13 μm (Figure 2a). Individual nanowires have a diameter of about 100 nm; however, due to the significant thickness of the SiNW layer, the nanowires tend to adhere to one another, forming agglomerates. These agglomerates measure approximately 1–2 μm in size, with an average spacing of about 1 μm between them (Figure 2b).

The current-voltage characteristics were linear in the range up to 10 V. The change in conductivity with the addition of bacteria was determined at a bias voltage of 6 V, since at this bias the current has the most "convenient" value for measurement over the entire range of bacterial concentrations. The dependencies described below exhibit similar behavior at various bias voltages within the linear region of the current-voltage characteristic. Therefore, the data for a bias voltage of 6 V are presented here as representative.

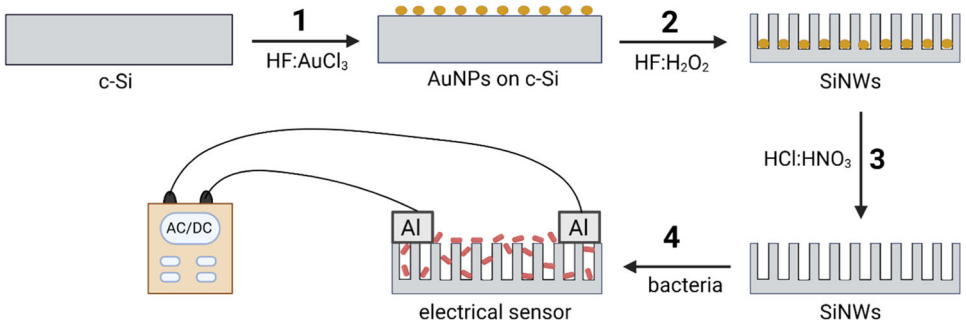

FIGURE 1 | Schematic representation of the preparation of an SiNW-based electrical sensor.

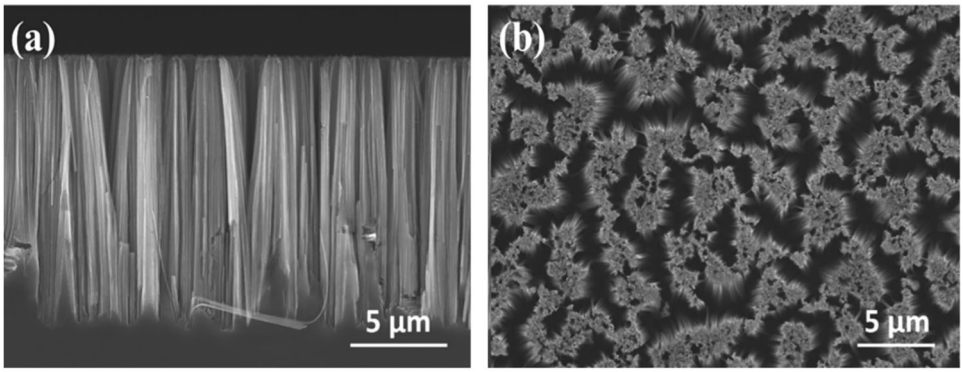

FIGURE 2 | SEM micrographs of an SiNWs sample: (a) side view, (b) top view.

To gain a deeper understanding of the charge transfer mechanisms in the SiNWs-bacteria system within distilled water, AC measurements were conducted. Figure 3 shows the impedance hodographs for SiNW samples at different concentrations of *L. innocua* bacteria (0, 10^5, 10^6, and 10^7 CFU/mL). The data are approximated using an equivalent circuit comprising a series resistor (R_1), a parallel resistor (R_2), and a capacitor (C). The real ($Re\,Z$) and imaginary ($-Im\,Z$) parts of the impedance change with varying bacterial concentrations. The formulas for the impedance Z and the hodograph of the proposed equivalent circuit are as follows:

$$Z = R_1 + \left(\frac{1}{R_2} + i\omega C\right)^{-1} = R_1 + \frac{R_2}{1 + (\omega C R_2)^2} - i\frac{\omega C R_2^2}{1 + (\omega C R_2)^2} \quad (1)$$

$$\left(\mathrm{Re}\quad Z - \left[R_1 + \frac{R_2}{2}\right]\right)^2 + (\mathrm{Im}\quad Z)^2 = \left(\frac{R_2}{2}\right)^2 \quad (2)$$

In this equivalent circuit, resistor R_1 represents the resistance between the sputtered contacts and the SiNWs, while resistor R_2 corresponds to the resistance of the SiNWs. The capacitor C_2 accounts for the polarization processes occurring in the space between the nanowires, which is filled with water and bacteria, as well as the capacitance of the boundaries between the nanocrystals composing the SiNWs.

The approximation curves, shown in Figure 3 as red lines, align with the theoretical model. Similar associations between physical processes and elements of equivalent circuits are commonly employed in the study of the electrical properties of nanocrystalline semiconductors (Barsoukov and Macdonald 2005).

The measured values of the real and imaginary parts of the impedance were sufficiently high to ensure accurate measurements using the available equipment. However, the impedance was measured with good accuracy only at higher frequencies, where the signal-to-noise ratio was more favorable. At higher frequencies, the hodograph follows a counterclockwise trajectory along the points in Figure 3, with a corresponding reduction in the real part of the impedance. Consequently, the first quarter of the semicircle, corresponding to lower frequencies and higher values of real impedance as predicted by Equation (2), is not visible.

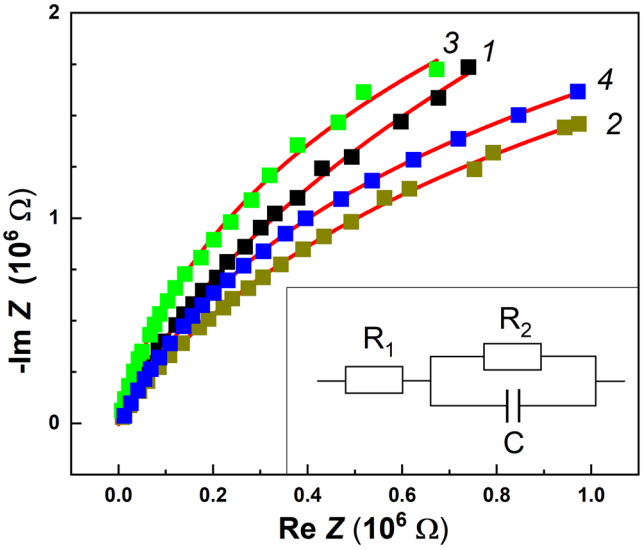

FIGURE 3 | Impedance hodographs of SiNW samples with the addition of distilled water containing different concentrations of *L. innocua* bacteria. The numbers on the graph correspond to the bacterial concentration: 1 – no bacteria (control), 2 – 10^5 CFU/mL, 3 – 10^6 CFU/mL, 4 – 10^7 CFU/mL. Red lines represent the approximation of the experimental data using the equivalent circuit shown in the inset.

The dependencies indicate that the addition of bacteria into the space between the nanowires alters the resistance R_2 and capacitance C, leading to nonlinear impedance changes. At low bacterial concentrations (10^5 CFU/mL), there is a slight decrease in impedance compared with the control sample (0 CFU/mL), likely due to insufficient filling of the space between the nanowires (Figure 4a,b). As the concentration increases (10^6 and 10^7 CFU/mL), bacteria begin to form coatings also on the surface of the SiNWs (Figure 4c,d), increasing both the resistance R_2 and the capacitance C, which results in higher real and imaginary impedance values.

Thus, the complex dependence of impedance on bacterial concentration is driven by competing effects involving changes in the resistance of the nanowires R_2 and the capacitive component C of the structure. These changes confirm the high sensitivity of the sensor to varying levels of bacterial contamination.

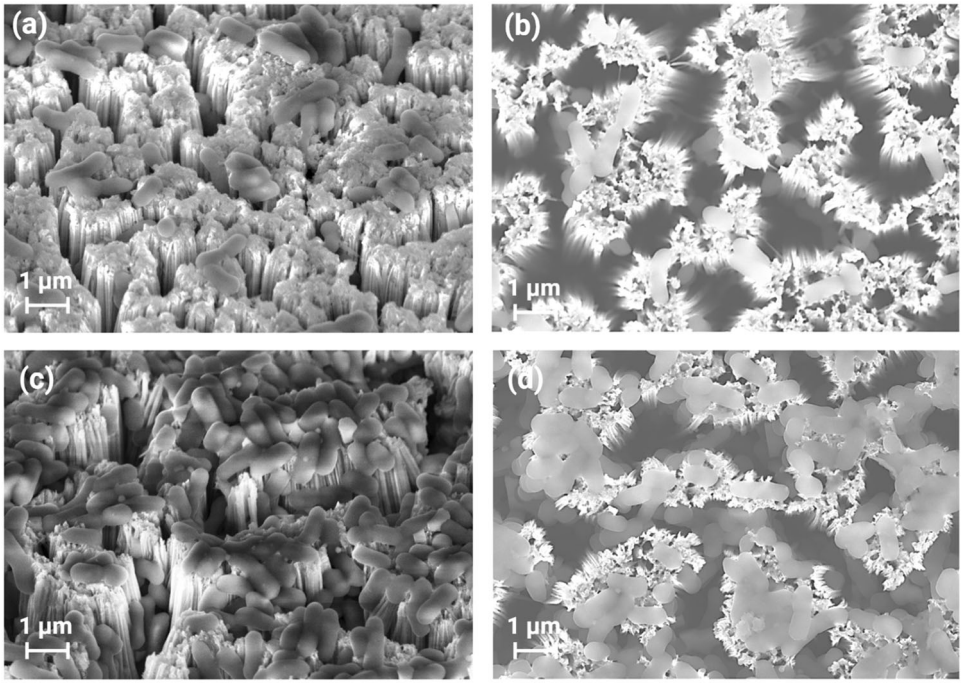

FIGURE 4 | SEM micrographs of SiNWs with adsorbed *L. innocua* at concentrations of (a, b) 10^5 CFU/mL and (c, d) 10^7 CFU/mL. Images (a, c) show a 45° tilt view, while (b, d) show a top view.

From Equation (1), we derive an expression for the conductance $G(\omega)$ as follows:

$$G(\omega) = \mathrm{Re}\left(\frac{1}{Z}\right) = \frac{1 + \frac{R_1}{R_2} + \omega^2 R_1 R_2 C^2}{\frac{(R_1 + R_2)^2}{R_2} + R_2(\omega R_1 C)^2} \tag{3}$$

Figure 5 shows the frequency dependence of conductance for SiNW samples exposed to *L. innocua* bacteria at a concentration of 10^6 CFU/mL. Similar frequency dependencies were observed for other bacterial concentrations. The conductance exhibits a consistent increase with frequency and is well approximated by Equation (3), as indicated by the quadratic relationship represented by the red line.

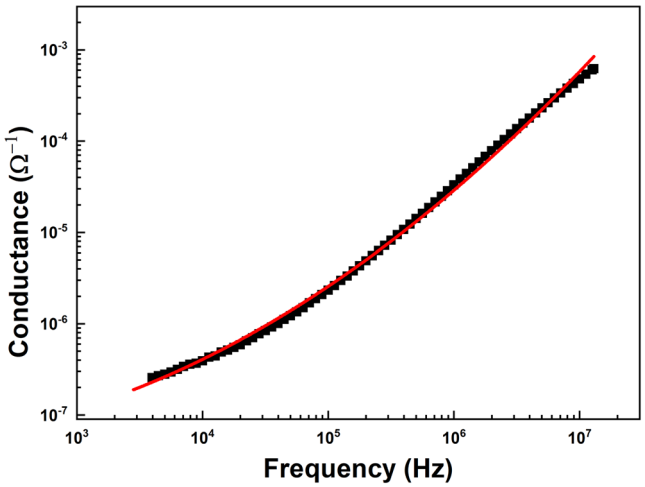

FIGURE 5 | Frequency dependence of conductance for SiNWs with *L. innocua* bacteria at a concentration of 10^6 CFU/ml (black squares) and its approximation by quadratic law (red line).

The c-Si substrate used in this study has dimensions of 5 × 5 cm and a resistivity of 10–20 Ω·cm, corresponding to a conductivity of 0.05–0.1 S/cm. Given the geometry of the experimental setup, where the distance between the electrical contacts is significantly smaller than the substrate dimensions, the conductance of the c-Si substrate between the contacts is calculated to be approximately 0.005–0.01 Ω^{-1}. This value is several orders of magnitude higher than the conductance of the SiNWs, which is on the order of 10^{-6} Ω^{-1}. As such, the contribution of the c-Si substrate to the measured conductance is negligible, ensuring that the recorded values accurately reflect the conductance of the SiNW array alone. This highlights the reliability of the method and confirms that the substrate does not introduce measurement artifacts.

Figure 6 illustrates the change in conductance under DC and AC conditions as a function of bacterial concentration on SiNWs, ranging from 10^5 to 10^7 CFU/mL. AC conductance measurements were performed at a frequency of 10 kHz, as the dependence on bacterial concentration stabilizes at higher frequencies. Additionally, conducting measurements at higher frequencies is less practical due to increased labor intensity.

As shown in Figure 6, increasing bacterial concentration from 10^5 to 10^7 CFU/mL results in a more than 10-fold rise in conductance for both DC and AC measurements. The AC conductance follows a similar trend to DC conductance, with an initial rapid increase at lower bacterial concentrations and a saturation effect as the concentration approaches 10^7 CFU/mL. However, AC conductance values are consistently higher than DC conductance across the entire concentration range,

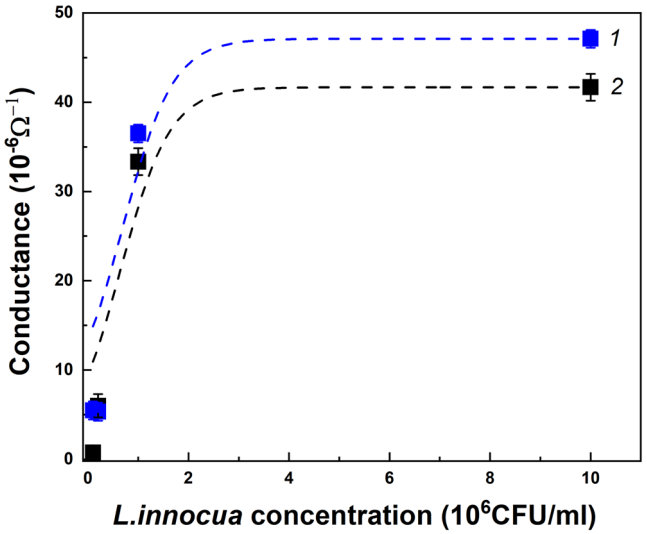

FIGURE 6 | Dependence of SiNW conductance at AC (blue squares, curve 1) and DC (black squares, curve 2) on *L. innocua* concentration. AC measurements were performed at 10 kHz. Error bars represent the range of 2–4 independent measurements performed for each bacterial concentration to ensure data reproducibility.

reflecting the enhanced sensitivity of the system to AC at the chosen frequency (10 kHz). This difference can be attributed to the reduced influence of potential barriers during AC measurements, as oscillating electric fields enable charge carriers to more effectively overcome these barriers (Ilyin et al. 2015; Forsh et al. 2008; Ilin et al. 2019). The observed saturation at 10^7 CFU/mL for both DC and AC conditions indicates the limited capacity of the nanowire system to further enhance conductance under these conditions.

4 | Conclusion

In this study, we demonstrated the feasibility of detecting *L. innocua* bacteria using a resistive method based on SiNW arrays. These arrays, consisting of vertically oriented SiNWs approximately 13 μm in length and 100 nm in diameter, exhibited high sensitivity to bacterial adsorption. Our findings revealed significant changes in the conductance of SiNWs when exposed to *L. innocua*, enabling detection at concentrations as low as 10^5 CFU/mL. Conductance increased more than 10-fold as bacterial concentration rose from 10^5 to 10^7 CFU/mL, with a clear saturation effect at higher concentrations. Both DC and AC measurements confirmed the nonlinear relationship between bacterial concentration and conductance, with AC conductance consistently higher than DC conductance, reflecting the reduced influence of potential barriers under AC conditions.

This study also introduced an equivalent circuit model that effectively describes the impedance behavior of the SiNW-bacteria system. The model and derived analytical expressions for impedance and the frequency dependence of conductance provided valuable insights into charge transport mechanisms in the presence of bacteria.

While the results underscore the promise of SiNWs for bacterial detection, several limitations must be acknowledged. First, the study was conducted using *L. innocua* as a model organism, which is nonpathogenic and less representative of more challenging clinical pathogens like *L. monocytogenes*. Future research should include pathogenic strains to validate the method's clinical applicability. Second, the experimental setup relies on distilled water as the medium, which simplifies the system but may not fully replicate real-world biological fluids, where matrix effects could influence sensor performance. Lastly, the fabrication of SiNW arrays, while relatively straightforward, may require further optimization to enhance scalability and reduce variability across samples.

Despite these limitations, the results highlight the potential of SiNW-based sensors as cost-effective, high-performance tools for bacterial detection. The principles demonstrated in this study pave the way for the development of advanced diagnostic devices suitable for clinical, environmental, and food safety applications.

Author Contributions

Alexander S. Ilin: conceptualization, data curation, methodology, writing – original draft. **Mikhail N. Martyshov:** software, supervision. **Dmitrii V. Gusev:** investigation, formal analysis, data curation. **Daniil M. Rusakov:** formal analysis, data curation. **Daria A. Nazarovskaia:** investigation. **Pavel A. Domnin:** methodology, investigation. **Mengyuan Wang:** investigation. **Ilia I. Tsiniaikin:** validation, investigation. **Kirill A. Gonchar:** funding acquisition, resources, writing – review and editing. **Svetlana A. Ermolaeva:** investigation, resources. **Liubov A. Osminkina:** writing – review and editing, conceptualization, project administration. **Pavel A. Forsh:** conceptualization, project administration. All authors have given approval to the final manuscript.

Acknowledgments

The authors gratefully acknowledge the Educational and Methodological Center of Lithography and Microscopy and Multiple Access Center of Lomonosov Moscow State University for providing the equipment. The study was supported by the Russian Science Foundation, grant no. 22-72-10062. https://rscf.ru/en/project/22-72-10062/.

Conflicts of Interest

The authors declare no conflicts of interest.

Data Availability Statement

The data that support the findings of this study are available on request from the corresponding author. The data are not publicly available due to privacy or ethical restrictions.

References

Ahmed, A., J. V. Rushworth, N. A. Hirst, and P. A. Millner. 2014. "Biosensors for Whole-Cell Bacterial Detection." *Clinical Microbiology Reviews* 27: 631–646. https://doi.org/10.1128/CMR.00120-13.

Allerberger, F., and M. Wagner. 2010. "Listeriosis: A Resurgent Foodborne Infection." *Clinical Microbiology and Infection* 16, no. 1: 16–23. https://doi.org/10.1111/j.1469-0691.2009.03109.x.

Archer, M., M. Christophersen, and P. M. Fauchet. 2005. "Electrical Porous Silicon Chemical Sensor for Detection of Organic Solvents." *Sensors and Actuators B: Chemical* 106, no. 1: 347–357. https://doi.org/10.1016/j.snb.2004.08.016.

Barsoukov, E., and J. R. Macdonald. 2005. *Impedance Spectroscopy: Theory, Experiment, and Applications*. John Wiley & Sons, Inc. https://doi.org/10.1002/0471716243.

De Boer, B. M., J. A. H. M. Kahlman, T. P. G. H. Jansen, H. Duric, and J. Veen. 2007. "An Integrated and Sensitive Detection Platform for Magneto-Resistive Biosensors." *Biosensors and Bioelectronics* 22, no. 9–10: 2366–2370. https://doi.org/10.1016/j.bios.2006.09.020.

Le Borgne, B., L. Pichon, A. C. Salaun, et al. 2018. "Bacteria Electrical Detection Using 3D Silicon Nanowires Based Resistor." *Sensors and Actuators B: Chemical* 273: 1794–1799. https://doi.org/10.1016/j.snb.2018.07.101.

Chalenko, Y. M., E. V. Sysoliatina, E. V. Kalinin, K. A. Sobianin, and S. A. Ermolaeva. 2017. "Natural Variants of Listeria Monocytogenes Internalin B With Different Ability to Stimulate Cell Proliferation and Cytoskeleton Rearrangement in Hep-2 Cells." *Molecular Genetics Microbiology and Virology* 32: 53–86. https://doi.org/10.3103/S0891416817020021.

Daraee, H., A. Eatemadi, E. Abbasi, S. Fekri Aval, M. Kouhi, and A. Akbarzadeh. 2016. "Application of Gold Nanoparticles in Biomedical and Drug Delivery." *Artificial Cells, Nanomedicine, and Biotechnology* 44: 410–422. https://doi.org/10.3109/21691401.2014.955107.

Feng, P., Y. Kong, M. Liu, S. Peng, and C. Shuai. 2021. "Dispersion Strategies for Low-Dimensional Nanomaterials and Their Application in Biopolymer Implants." *Materials Today Nano* 15: 100127. https://doi.org/10.1016/j.mtnano.2021.100127.

Filatova, D., and M. Rumyantseva. 2023. "Additives in Nanocrystalline Tin Dioxide: Recent Progress in the Characterization of Materials for Gas Sensor Applications." *Materials* 16: 6733. https://doi.org/10.3390/ma16206733.

Flammini, A., D. Marioli, and A. Taroni. 2004. "A Low-Cost Interface to High-Value Resistive Sensors Varying Over a Wide Range." *IEEE Transactions on Instrumentation and Measurement* 53, no. 4: 1052–1056. https://doi.org/10.1109/TIM.2004.831500.

Forsh, P. A., M. N. Martyshov, A. P. Latysheva, A. S. Vorontsov, V. Y. Timoshenko, and P. K. Kashkarov. 2008. "Mobility of Charge Carriers in Porous Silicon Layers." *Journal of Experimental and Theoretical Physics* 107: 1022–1026. https://doi.org/10.1134/S106377610812011X.

Forsh, P. A., M. N. Martyshov, V. Y. Timoshenko, and P. K. Kashkarov. 2007. "Impedance Spectroscopy of In-Plane Anisotropic Porous Silicon Films." *Physica Status Solidi C* 4, no. 6: 1981–1985. https://doi.org/10.1002/pssc.200674347.

Gonchar, K. A., S. N. Agafilushkina, D. V. Moiseev, et al. 2020. "H1N1 Influenza Virus Interaction With a Porous Layer of Silicon Nanowires." *Materials Research Express* 7: 035002. https://doi.org/10.1088/2053-1591/ab7719.

Gongalsky, M. B., U. A. Tsurikova, J. V. Samsonova, et al. 2020. "Double Etched Porous Silicon Nanowire Arrays for Impedance Sensing of Influenza Viruses." *Results in Materials* 6: 100084. https://doi.org/10.1016/j.rinma.2020.100084.

Gupta, A. K., and M. Gupta. 2005. "Synthesis and Surface Engineering of Iron Oxide Nanoparticles for Biomedical Applications." *Biomaterials* 26: 3995–4021. https://doi.org/10.1016/j.biomaterials.2004.10.012.

Ilin, A. S., V. M. Gololobov, E. A. Forsh, P. A. Forsh, and P. K. Kashkarov. 2019. "Calculation of the Grain Potential Barrier in the Poly– and Nanocrystalline Semiconductors." *Materials Science and Engineering* 20: 122–128. https://doi.org/10.17073/1609-3577-2017-2-122-128.

Ilin, A. S., M. I. Ikim, P. A. Forsh, et al. 2017. "Green Light Activated Hydrogen Sensing of Nanocrystalline Composite ZnO-In_2O_3 Films at Room Temperature." *Scientific Reports* 7: 12204. https://doi.org/10.1038/s41598-017-12547-5.

Ilyin, A. S., N. P. Fantina, M. N. Martyshov, et al. 2015. "Voltage Effect on the Sensitivity of Nanocrystalline Indium Oxide to Nitrogen Dioxide Under Ultraviolet Irradiation." *Technical Physics Letters* 41: 252–254. https://doi.org/10.1134/S1063785015030074.

Ireton, K., R. Mortuza, G. C. Gyanwali, A. Gianfelice, and M. Hussain. 2021. "Role of Internalin Proteins in the Pathogenesis of Listeria Monocytogenes." *Molecular Microbiology* 116, no. 6: 1407–1419. https://doi.org/10.1111/mmi.14836.

Ivnitski, D., I. Abdel-Hamid, P. Atanasov, and E. Wilkins. 1999. "Biosensors for Detection of Pathogenic Bacteria." *Biosensors and Bioelectronics* 14: 599–624. https://doi.org/10.1016/S0956-5663(99)00039-1.

Jeong, H. E., I. Kim, P. Karam, H. J. Choi, and P. Yang. 2013. "Bacterial Recognition of Silicon Nanowire Arrays." *Nano Letters* 13, no. 6: 2864–2869. https://doi.org/10.1021/nl401205b.

Kotsiri, Z., J. Vidic, and A. Vantarakis. 2022. "Applications of Biosensors for Bacteria and Virus Detection in Food and Water—A Systematic Review." *Journal of Environmental Sciences* 111: 367–379. https://doi.org/10.1016/j.jes.2021.04.009.

Levitsky, I. 2015. "Porous Silicon Structures as Optical Gas Sensors." *Sensors* 15, no. 8: 19968–19991. https://doi.org/10.3390/s150819968.

Lopes-Luz, L., M. Mendonça, M. Bernardes Fogaça, A. Kipnis, A. K. Bhunia, and S. Bührer-Sékula. 2021. "Listeria Monocytogenes: Review of Pathogenesis and Virulence Determinants-Targeted Immunological Assays." *Critical Reviews in Microbiology* 47, no. 5: 647–666. https://doi.org/10.1080/1040841X.2021.1911930.

Martyshov, M. N., P. A. Forsh, V. Y. Timoshenko, and P. K. Kashkarov. 2009. "Electrical Conductivity in Anisotropic Porous Silicon Films." *Journal of Nanoelectronics and Optoelectronics* 4, no. 1: 134–136. https://doi.org/10.1166/jno.2009.1012.

Nazarovskaia, D. A., P. A. Domnin, O. D. Gyuppenen, et al. 2023. "Advanced Bacterial Detection With SERS-Active Gold- and Silver-Coated Porous Silicon Nanowires." *Bulletin of the Russian Academy of Sciences: Physics* 87, no. Suppl. 1: S41–S46. https://doi.org/10.1134/S1062873823704385.

Oevermann, A., A. Zurbriggen, and M. Vandevelde. 2010. "Rhombencephalitis Caused by Listeria Monocytogenes in Humans and Ruminants: A Zoonosis on the Rise?" *Interdisciplinary Perspectives on Infectious Diseases* 2010: 632513. https://doi.org/10.1155/2010/632513.

Osminkina, L. A., S. N. Agafilushkina, E. A. Kropotkina, et al. 2022. "Antiviral Adsorption Activity of Porous Silicon Nanoparticles Against Different Pathogenic Human Viruses." *Bioactive Materials* 7: 39–46. https://doi.org/10.1016/j.bioactmat.2021.06.001.

Xu, H., H. Shang, C. Wang, and Y. Du. 2020. "Low-Dimensional Metallic Nanomaterials for Advanced Electrocatalysis." *Advanced Functional Materials* 30, no. 50: 2006317. https://doi.org/10.1002/adfm.202006317.

Zhang, X., S. Wang, X. Chen, and C. Qu. 2021. "Controlling Listeria Monocytogenes in Ready-To-Eat Meat and Poultry Products: An Overview of Outbreaks, Current Legislations, Challenges, and Future Prospects." *Trends in Food Science & Technology* 116: 24–35. https://doi.org/10.1016/j.tifs.2021.07.014.